Description of the ARM Large-Scale Forcing Data from the Constrained Variational Analysis (VARANAL) Version 2

S Tang   C Tao
S Xie   M Zhang

August 2019

DISCLAIMER

This report was prepared as an account of work sponsored by the U.S. Government. Neither the United States nor any agency thereof, nor any of their employees, makes any warranty, express or implied, or assumes any legal liability or responsibility for the accuracy, completeness, or usefulness of any information, apparatus, product, or process disclosed, or represents that its use would not infringe privately owned rights. Reference herein to any specific commercial product, process, or service by trade name, trademark, manufacturer, or otherwise, does not necessarily constitute or imply its endorsement, recommendation, or favoring by the U.S. Government or any agency thereof. The views and opinions of authors expressed herein do not necessarily state or reflect those of the U.S. Government or any agency thereof.

Description of the ARM Large-Scale Forcing Data from the Constrained Variational Analysis (VARANAL) Version 2

S Tang, Lawrence Livermore National Laboratory (LLNL)
C Tao, LLNL
S Xie, LLNL
M Zhang, Stony Brook University

August 2019

Acronyms and Abbreviations

3DCVA	three-dimensional constrained variational analysis
ABRFC	Arkansas-Red Basin River Forecast Center
ADC	ARM Data Center
ADI	ARM Data Integrator
AMIE-GAN	ARM Madden-Julian Oscillation (MJO) Investigation Experiment-Gan Island
ARM	Atmospheric Radiation Measurement
BAEBBR	Bulk Aerodynamic Technique EBBR value-added product
CLASIC	Cloud and Land Surface Interaction Campaign
CRM	cloud-resolving model
CSU	Colorado State University
DOI	digital object identifier
DYNAMO	Dynamics of the Madden-Julian Oscillation
EBBR	energy balance Bowen ratio
ECMWF	European Centre for Medium-Range Weather Forecasts
ECOR	eddy correlation flux measurement system
GOES	Geostationary Operational Environment Satellite
IOP	intensive operational period
ISDAC	Indirect and Semi-Direct Aerosol Campaign
LES	large-eddy simulation
LH	latent heat
LLNL	Lawrence Livermore National Laboratory
LWP	liquid water path
M3CE	Midlatitude Continental Convective Clouds
MAO	ARM's Mobile Facility site at Manacapuru, Brazil during GoAmazon 2014/15
MERRA	Modern Era-Retrospective Analysis for Research and Applications
M-PACE	Mixed-Phase Arctic Cloud Experiment
MWR	microwave radiometer
NOAA	National Oceanic and Atmospheric Administration
NSA	North Slope of Alaska
NWP	numerical weather prediction
PECAN	Plains Elevated Convection at Night
QCECOR	Quality-Controlled ECOR value-added product
RAP	Rapid Refresh
RUC	Rapid Update Cycle
SCM	single-column model

SGP	Southern Great Plains
SH	sensible heat
SIPAM	Sistema de Proteção da Amazônia (Amazon Protection System) radar
SIROS	solar and infrared observing system
SMART-R	Shared Mobile Atmospheric Research and Teaching Radar
SMOS	surface meteorological observation station
S-POL	S-band dual-polarimetric radar
TOA	top of atmosphere
TOGA	Tropical Ocean Global Atmosphere
TRMM	Tropical Rainfall Measuring Mission
TWP	Tropical Western Pacific
TWP-ICE	Tropical Warm Pool-International Cloud Experiment
VAP	value-added product
VARANAL	variational analysis

Contents

Figures

Tables

1.0 Introduction

1.1 General Description

This technical report represents an update of the previous technical report written by Zhang et al. (2001a) (available at http://www.arm.gov/publications/tech_reports/arm-tr-005.pdf), which described the U.S. Department of Energy Atmospheric Radiation Measurement (ARM) user facility constrained variational analysis (VARANAL) that is used to develop the large-scale forcing data for driving single-column models (SCMs), cloud-resolving models (CRMs), and large-eddy simulation models (LES). The VARANAL algorithm was originally developed by Zhang and Lin (1997) and Zhang et al. (2001b) at Stony Brook University and was migrated to the Lawrence Livermore National Laboratory (LLNL) as the ARM operational objective analysis system in May 1999. Since then, the algorithm has been evolved with time along with the availability of new observations and techniques to meet various modeling needs. Major updates include:

1. The method used to develop multi-year continuous forcing data (Xie et al. 2004),

2. The incorporation of eddy correlation flux measurement system (ECOR) turbulent fluxes into the analysis (Tang et al. 2019), and

3. Improvements to the workflow (e.g., implementing part of the code into the ARM Data Integrator [ADI]) to increase efficiency.

The ARM large-scale forcing data have been widely used for SCM/CRM/LES to understand and improve physical processes in models. Zhang et al. (2016) has provided a comprehensive review of the SCM concept, early efforts to derive forcing data for SCM studies, efforts of the ARM constrained variational analysis, and previous SCM studies using ARM cases. This technical report focuses on the constrained variational analysis algorithm and the introduction of the ARM VARANAL products.

We also extended the VARANAL algorithm into a three-dimensional constrained variational analysis (3DCVA) (Tang and Zhang 2015) and designed an ensemble framework (Tang et al. 2016a) to address the forcing uncertainty. The 3D large-scale forcing data are released as another datastream named "varanal3d". Please refer to the ARM varanal3d technical report for more information (https://www.arm.gov/capabilities/vaps/varanal3d).

1.2 Data Information

The current large-scale forcing data sets archived by ARM includes two major products:

1. Radiosonde- or numerical weather prediction (NWP)-based forcing data for short-term intensive operational periods (IOPs) at different ARM observatories or mobile sites.

2. The multi-year continuous forcing data at the ARM observatories.

A full list of large-scale forcing data for the ARM field campaigns is provided in Section 4.

All the VARANAL forcing data share the same doi: **doi:10.5439/1273323**. They are available to the community from the ARM Data Center (http://www.archive.arm.gov/discovery/). To cite the data, please refer to Zhang and Lin (1997) and Zhang et al. (2001b) for the VARANAL algorithm and the sounding-based IOP forcing, Xie it al. (2004) for the numerical weather prediction (NWP)-based IOP, and Xie et al. (2004) and Tang et al. (2019) for the continuous forcing data at ARM's Southern Great Plains (SGP) atmospheric observatory. For major field campaigns, also refer to the references shown in Section 4. For questions, please contact Shuaiqi Tang (tang32@llnl.gov), Cheng Tao (tao4@llnl.gov), or Shaocheng Xie (xie2@llnl.gov).

2.0 Algorithm

The constrained variational analysis method was developed by Zhang and Lin (1997) to derive large-scale vertical velocity and advective tendencies from sounding measurements of winds, temperature, and water vapor mixing ratio over a network of a small number of stations. Here, we briefly review the algorithm of the constrained variational analysis that was introduced in Zhang and Lin (1997) and Zhang et al. (2001b). We also provide details on the NWP-based ARM continuous forcing data at SGP and the version updates as discussed in Xie et al. (2004) and Tang et al. (2019).

2.1 Theoretical Formulation

From Zhang and Lin (1997), the vertical integration of the atmospheric mass, moisture, dry static energy, and momentum equations in an atmospheric column (Figure 1) are:

$$\left\langle \nabla \cdot \vec{V} \right\rangle = -\frac{1}{g}\frac{dP_s}{dt} \tag{1}$$

$$\frac{\partial \left\langle q \right\rangle}{\partial t} + \left\langle \nabla \cdot \vec{V} q \right\rangle = E_s - P_{rec} - \frac{\partial \left\langle q_l \right\rangle}{\partial t} + \frac{\omega_s q_s}{g} \tag{2}$$

$$\frac{\partial \left\langle s \right\rangle}{\partial t} + \left\langle \nabla \cdot \vec{V} s \right\rangle = R_{TOA} - R_{SRF} + L_v P_{rec} + SH + L_v \frac{\partial \left\langle q_l \right\rangle}{\partial t} + \frac{\omega_s s_s}{g} \tag{3}$$

$$\frac{\partial \left\langle \vec{V} \right\rangle}{\partial t} + \left\langle \nabla \cdot \vec{V} \vec{V} \right\rangle + f \vec{k} \times \left\langle \vec{V} \right\rangle + \nabla \left\langle \phi \right\rangle = \vec{\tau_s} \tag{4}$$
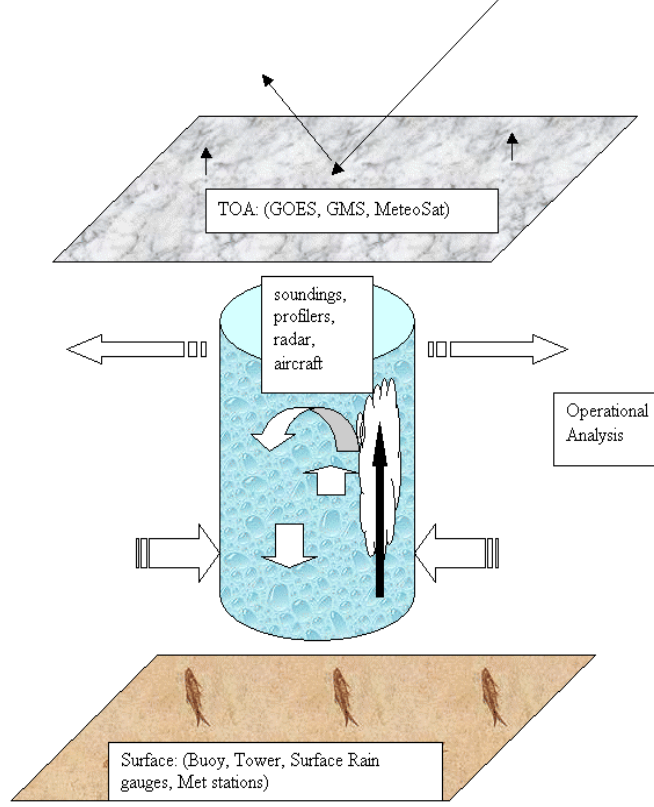
Figure 1.   Schematic figure of an atmospheric column in VARANAL.

where the bracket <*> represents vertical integration from the surface to the top of atmosphere (TOA); $\vec{V}$ is wind vector in isobaric surface; g is gravitational constant; P_s is surface pressure, q is water vapor mixing ratio; $s = C_p T + gz$ is the dry static energy; E_s is surface evaporation; P_{rec} is surface precipitation; L_v is the latent heat of vaporization; q_l is cloud liquid water content; R_{TOA} and R_{SRF} are net downward radiation at TOA and surface; ω_s, q_s, and s_s are the pressure vertical velocity, water vapor mixing ratio, and dry static energy at the surface, respectively; SH is surface sensible heat flux; f is the Coriolis parameter; $\vec{k}$ is the unit vector in vertical direction; ϕ is the geopotential, and $\vec{\tau}_s$ is the surface wind stress. Ice processes and advection of cloud hydrometeors are neglected. The terms related with ω_s are from the vertical integration of the three-dimensional divergence terms. Physically, they represent the change of column moisture and column energy purely due to the change of column mass.

In the constrained variational analysis method, the atmospheric variables ($\vec{V}$, s, q) are forced to satisfy Equations (1)-(4) with minimum adjustments to the first guess (either from radiosonde or from NWP analysis). The final analysis product is derived by minimizing the cost function:

$$I(t) = \iiint_{p,x,y} \left[\alpha_u \left(u - u_o\right)^2 + \alpha_v \left(v - v_o\right)^2 + \alpha_q \left(q - q_o\right)^2 + \alpha_s \left(s - s_o\right)^2 \right] dxdydp$$

(5)

with Equations (1)-(4) as strong constraints, where u, v, q, s denote the final analysis data, u_o, v_o q_o, s_o denote the first guess, and α is the weighting function related to the error estimates in the initial first guess.

2.2   Numerical Implementation

For N stations in the sounding network, each with K layers, we use x_{ik} to denote a state variable at station i and layer k, and use column vector X to denote variables u, v, q, s at all grids:

$$X^T = [x_{11}, x_{12},..., x_{1k}, x_{21},..., x_{ik},..., x_{NK}]$$

(6)

Where superscript T means transpose of vector. The cost function (5) can be written as

$$I(t) = (u-u_o)^T W_u^{-1} (u-u_o) + (v-v_o)^T W_v^{-1} (v-v_o) + (q-q_o)^T W_q^{-1} (q-q_o) + (s-s_o)^T W_s^{-1} (s-s_o)$$

(7)

Where W is the weighting matrix related with the error covariance of a variable. The strong constraints of Equations (1)-(4) can be written in the discrete form:

$$A_{mass} = \left\langle \left(\nabla \cdot \vec{V} \right)_m \right\rangle + \frac{1}{g} \left(\frac{dP_s}{dt} \right)_m = 0$$

(8)

$$A_{water} = \left\langle \left(\frac{\partial q}{\partial t} \right)_m \right\rangle + \left\langle \left(\nabla \cdot \vec{V} q \right)_m \right\rangle - E_s + P_{rec} + \left\langle \left(\frac{\partial q_l}{\partial t} \right)_m \right\rangle = 0$$

(9)

$$A_{heat} = \left\langle \left(\frac{\partial s}{\partial t} \right)_m \right\rangle + \left\langle \left(\nabla \cdot \vec{V} s \right)_m \right\rangle - R_{TOA} + R_{SRF} - L_v P_{rec} - SH - L_v \left\langle \left(\frac{\partial q_l}{\partial t} \right)_m \right\rangle = 0$$

(10)

$$A_{momentum} = \left\langle \left(\frac{\partial \vec{V}}{\partial t} \right)_m \right\rangle + \left\langle \left(\nabla \cdot \vec{V} \vec{V} \right)_m \right\rangle + f \vec{k} \times \left\langle \left(\vec{V} \right)_m \right\rangle + \left\langle \left(\nabla \phi \right)_m \right\rangle - \vec{\tau}_s = 0$$

(11)

Where

$$\left\langle X \right\rangle = \frac{1}{g} \sum_{k=1}^{k=K} \left(X_k \Delta P_k \right)$$

(12)

and subscript m represents average of the area covered by the N stations. The surface vertical velocity ω_s is assumed as 0. Geopotential height ϕ can be derived from the virtual temperature analysis using the hydrostatic balance

$$\frac{\partial \phi}{\partial p} = -\frac{RT_v}{P}$$

(13)

The variational equations for the analyzed variables are:

$$\frac{\partial I(t)}{\partial x_{ik}} + \lambda_1(t)\frac{\partial A_{mass}}{\partial x_{ik}} + \lambda_2(t)\frac{\partial A_{water}}{\partial x_{ik}} + \lambda_3(t)\frac{\partial A_{heat}}{\partial x_{ik}} + \lambda_{4,5}(t)\frac{\partial A_{momtentum}}{\partial x_{ik}} = 0$$

(14)

Where x_{ik} stands for variables of u_{ik}, v_{ik}, q_{ik}, s_{ik}. λ is the Lagrange multiplier. Note that $A_{momtentum}$ includes two equations for u and v, respectively. With a total of four variables and five Lagrange multipliers, the total number of variables to be calculated in any given time is $4 \times N \times K + 5$.

We assume measurement errors are uncorrelated at different locations and for different variables, so the covariance matrix W is diagonal. The diagonal elements are the reciprocal of error variances $\sigma_{x_{ik}}^2$. Thus, Equation (14) becomes:

$$2\sigma_{x_{ik}}^{-2}\left(x_{ik} - x_{o,ik}\right) + \lambda_1(t)\frac{\partial A_{mass}}{\partial x_{ik}} + \lambda_2(t)\frac{\partial A_{water}}{\partial x_{ik}} + \lambda_3(t)\frac{\partial A_{heat}}{\partial x_{ik}} + \lambda_{4,5}(t)\frac{\partial A_{momtentum}}{\partial x_{ik}} = 0$$

(15)

Or

$$x_{ik} = x_{o,ik} - \frac{\sigma_{x_{ik}}^2}{2}\left[\lambda_1(t)\frac{\partial A_{mass}}{\partial x_{ik}} + \lambda_2(t)\frac{\partial A_{water}}{\partial x_{ik}} + \lambda_3(t)\frac{\partial A_{heat}}{\partial x_{ik}} + \lambda_{4,5}(t)\frac{\partial A_{momtentum}}{\partial x_{ik}}\right]$$

(16)

Numerical calculation of Equation (16) and Equations (8)-(11) is carried out in an iterative mode. The iteration, when described to a single time level, contains three steps. The first step is that the previous estimate or original measurements are used to calculate each partial derivative to x_{ik} on the right-hand-side of Equation (16) using the formation of Equations (8)-(11).

$$x_{ik}^{(l)} = x_{o,ik} - \frac{\sigma_{x_{ik}}^2}{2}\sum_{n=1}^{5}\lambda_n(t)B_{n,ik}^{(l-1)}$$

(17)

Where l denotes the iteration index, $B_{n,ik}^{(l-1)}$ are the partial derivatives of constraints A. Substitution of Equation (17) to Equations (8)-(11) yields a linearized set of equations for λ_n. A general form of the equations is:

$$A_n\left(x_{o,ik} - \frac{\sigma_{x_{ik}}^2}{2}\sum_{n=1}^{5}\lambda_n(t)B_{n,ik}^{(l-1)}\right) = 0$$

(18)

Because of the linearity of the operator, it can be further written as:

$$A_n\left(x_{o,ik}\right) - \sum_{n=1}^{5}\left[\frac{\sigma_{x_{ik}}^2}{2}\lambda_n\left(t\right)A_n\left(B_{n,ik}^{(l-1)}\right)\right] = 0$$

(19)

This set of five equations for the five constraints is used to solve for λ_n at any given time. This constitutes the second step in the iteration.

In the third step, the adjustments are calculated by using the newly obtained λ_n in Equation (17). After that, the next iteration is performed.

Because the constraints of Equations (8)-(11) contain time derivatives, the actual iteration is carried out simultaneously for all time levels in the field experiment. For continuous forcing, it is carried out every month.

2.3 Applications to the ARM Data

The constrained variational analysis method is applied to various forms of ARM data to produce its value- added outputs.

2.3.1 Sounding-Based IOP Forcing

Many ARM sounding IOPs have a network of radiosondes launched to measure upper-level profiles of temperature, relative humidity, and winds. These measured upper-level data are analyzed with background fields from NWP analysis data or reanalysis data to get the upper-level profiles needed by the constrained variational analysis using an analysis scheme of Cressman (1959). A list of the sounding- based forcing products is shown in Section 4.

2.3.2 NWP-Based IOP Forcing

In the cases when radiosonde data are unavailable, NWP operational analysis or reanalysis data are used for the upper-level variables. Xie et al. (2004) found that the NWP-based forcing agreed well with the sounding-based forcing, especially during precipitation period when the constraint is strong. Previously used analysis/reanalysis data in the past ARM field campaigns include the Rapid Update Cycle (RUC)/Rapid Refresh (RAP) analysis, European Centre for Medium-Range Weather Forecasts (ECMWF) analysis, ERA-interim reanalysis, and Modern Era-Retrospective Analysis for Research and Applications (MERRA) reanalysis data. A list of the NWP-based forcing products is provided in Section 4.

2.3.3 Multi-Year Continuous Forcing at SGP

The multi-year continuous forcing is developed to run operationally at a site for a long time, other than running for a few weeks or months for a typical IOP. It has been derived at the ARM SGP site (1999- current), Tropical Western Pacific (TWP) site (wet seasons 2004-2006), and Brazilian Amazon (MAO) site (2014-2015). The continuous forcing at SGP is a major VARANAL product with long-term,

high-density surface measurements providing accurate constraints. The long-term continuous forcing product allows climatological analysis on physical processes using both observations and SCM/CRM/LES simulations.

Two versions of continuous forcing data products are currently available at the ARM SGP site: version 1 (Xie et al. 2004) available from 1999 to 2011 and version 2 (Tang et al. 2019) available from 2004 to October 2018. The major version update is that version 1 only uses energy balance Bowen ration (EBBR)-measured surface turbulence fluxes while version 2 uses merged fluxes from EBBR and ECOR to better represent various surface types within the analysis domain. Other updates cover such topics as fixing bugs, updating input data version, and optimizing workflow.

ECOR and EBBR are two instruments measuring surface turbulence fluxes in different ways. EBBR was deployed first SGP while ECOR was deployed later (reliable ECOR data at SGP are from September 2003). Details about the two instruments can be found in the ECOR and EBBR handbooks (Cook 2019a, b). Although there are value-added products (VAP) for both instruments, the Quality-Controlled ECOR (QCECOR) and Bulk Aerodynamic Technique EBBR (BAEBBR), available to correct the systematic instrumental biases or fill the missing gaps when the method is invalid, the turbulence fluxes measured from ECOR and EBBR still have quite significant differences. Overall, BAEBBR has larger latent heat (LH) and smaller sensible heat (SH) compared to QCECOR during summer. These differences are mainly due to the different surface vegetation types the instruments are representing, and partly due to the instrument difference itself. As a result, the derived large-scale forcing has quite considerable uncertainty (climatologically ~20% for vertical velocity) in magnitude (Figure 2) due to the difference of ECOR and EBBR. More details can be found in Tang et al. (2019).
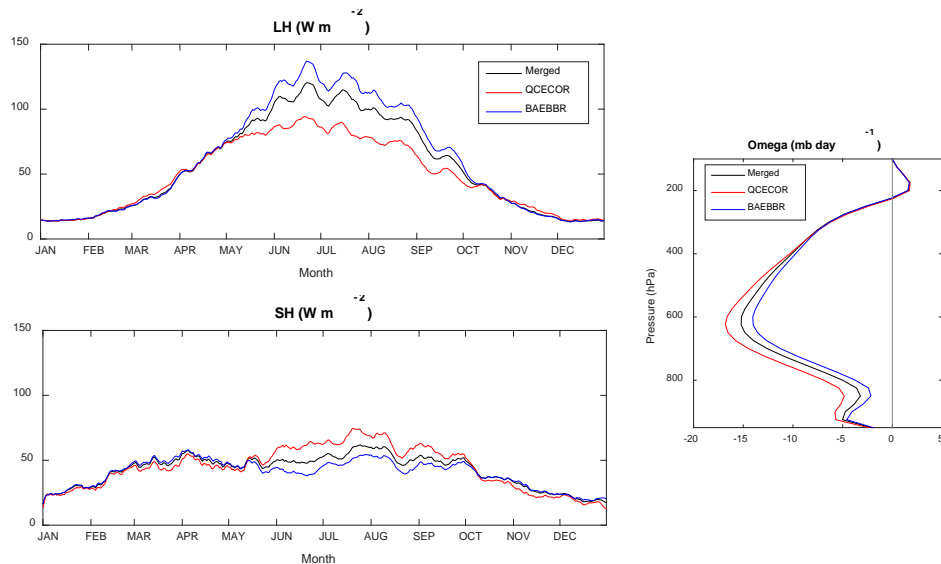

Figure 2.   The seasonal cycle of SGP domain-averaged latent heat (LH) and sensible heat (SH) fluxes by using QCECOR-only (QCECOR), BAEBBR-only (BAEBBR), and both QCECOR and BAEBBR data (merged) averaged from 2004-2015, and the impact to the derived large-scale vertical velocity (Omega). Revised from Tang et al. (2019).

3.0 Calculations

This section describes the operation of the algorithm, including its inputs and outputs.

3.1 Workflow

The structure of VARANAL for continuous forcing consists of four steps (Figure 3): (1) preparation of the required input data, (2) preprocess, (3) variational analysis, and (4) postprocess and output of final products. In step 1, all the required data are collected and reorganized from the original datastreams to output in a standard format for further analysis. Step 2 includes major quality control of the input data, averaging the data within the domain, filling in missing measurements, and interpolating to consistent observation time step. In step 3, the large-scale variables (u, v, T, q) are adjusted by the constrained variational analysis method and the large-scale advective tendencies and vertical velocity are calculated. Step 4 calculates and outputs the variables that will be used to force and evaluate SCM/CRM/LES.
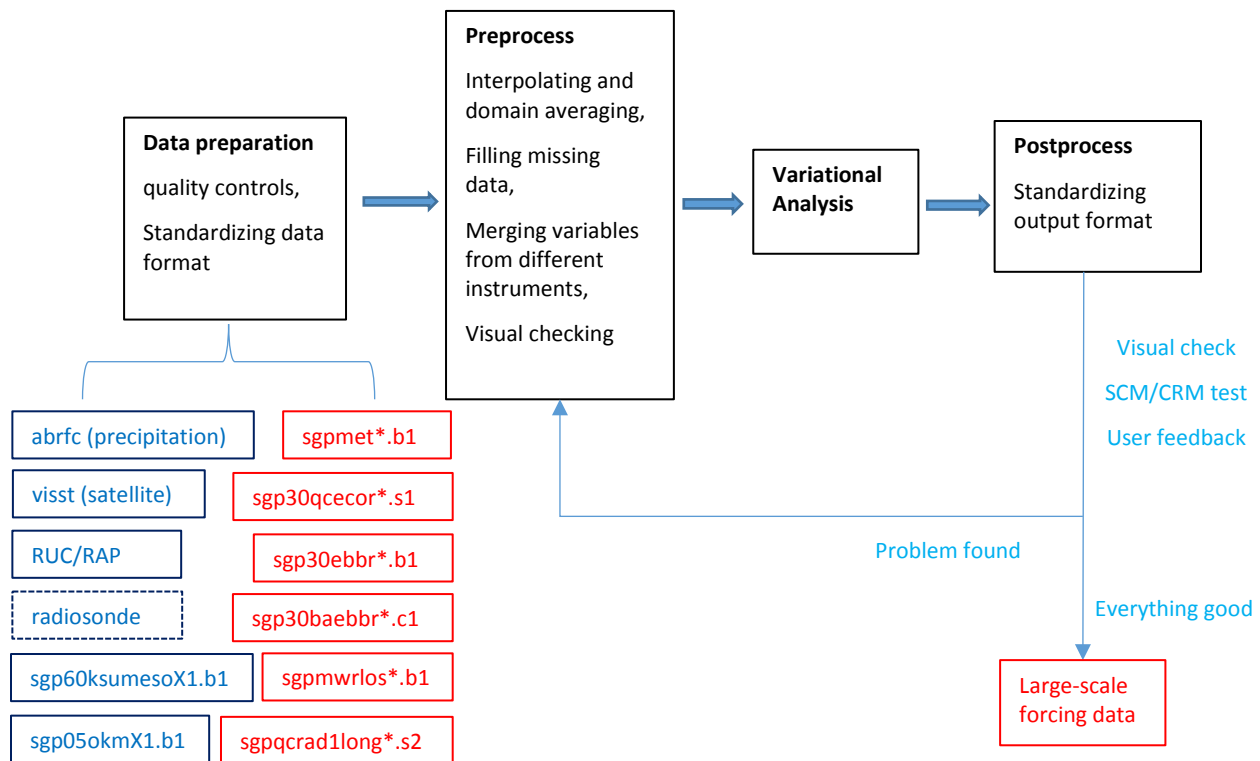
Figure 3. Illustration of the structure of the variational analysis system and the example of input datastreams for the ARM continuous forcing at SGP. The datastreams in red are ARM datastreams while those in blue (except radiosonde) represent data sets from external data centers and archived by ARM. Radiosonde is not used for continuous forcing but is used for some field campaigns.

For the large-scale forcing data at SGP, the input data sets include measurements from many instruments. A detailed description of the input data is given in Section 3.2. To increase the efficiency of the workflow and reduce human effort during the operational processes of the continuous forcing, a set of code optimizing efforts has been made. Step (1) has been implemented in the ARM Data Integrator (ADI) in

2017 to directly prepare data from the ARM Data Center. The visual checking part in step (2) is re-coded from interactive mode into offline iterative mode for more efficient human work. The workflow of step (3) and step (4) are optimized for less human interaction and standardizing output format. These efforts have greatly increased the automation of the framework and are more suitable for operational running of the continuous forcing with higher efficiency.

For the large-scale forcing for field campaigns, some incorporated radiosonde measurements while some used NWP analysis or reanalysis for the background data. Other surface input data may come from different data sources or are even unavailable. NWP analysis or reanalysis data are used when some input variables are unavailable. A brief description of input data sets used for each ARM field campaign is given in Section 4. More details of the VARANAL setup for major field campaigns can be found in the README file along with the forcing data at the ARM Data Center (https://iop.archive.arm.gov/arm-iop/0eval-data/xie/scm-forcing/) or on our website (https://portal.nersc.gov/project/capt/ARMVAP/varanal.html).

## 3.2 Input Data for Continuous Forcing

As an example of large-scale forcing data at the SGP site, the input data for current continuous forcing data are listed below:

- RUC/RAP (sgpruc20isobX1.c1/ sgprap20plevX1.c1): The National Oceanic and Atmospheric Administration (NOAA) Rapid Update Cycle (RUC, before May 2012) analysis and Rapid Refresh (RAP, after May 2012) analysis.

- SMOS (sgpmet**.b1): Surface meteorological observation stations measuring surface precipitation, surface pressure, surface winds, temperature, and relative humidity.

- EBBR (sgp30baebbr**.s1): Energy balance Bowen ratio stations measuring surface latent and sensible heat fluxes and surface broadband net radiative flux.

- ECOR (sgp30qcecor**.s1): Eddy correlation flux measurement systems measuring surface latent and sensible heat fluxes.

- OKM (sgp05okmX1.b1) and KAM (sgp60ksumesoX1.b1): Oklahoma and Kansas Mesonet stations measuring surface precipitation, pressure, winds, and temperature.

- MWR (sgpmwrlos**.b1): Microwave radiometer stations measuring the column precipitable water and total cloud liquid water.

- SIROS (sgpqcrad1long**.s2): Solar and infrared observing systems measuring broadband longwave and shortwave radiative fluxes.

- GOES (sgpvisstgridg13v4minnisX1.c1): the Geostationary Operational Environment Satellite measuring radiative fluxes at TOA.

- ABRFC (sgpabrfcprecipX1.c1): the 4-km-resolution gridded precipitation products from Arkansas-Red Basin River Forecast Center based on WSD-88 rain radar and gauge measurements.

The locations of these stations as of December 2015 are plotted in Figure 4. Along with time, there are some changes on the abbreviation or instrument (datastream) names. Datastream names may change for other time and versions. Station numbers and locations may also change in time (e.g., KAM data is only

available before September 2013 so they are not shown in Figure 4). These datastreams are also used for other field campaigns operated at the SGP site. A list of VARANAL products for field campaigns at SGP are given in Section 4.

VARANAL Domain at SGP (Dec. 2015)
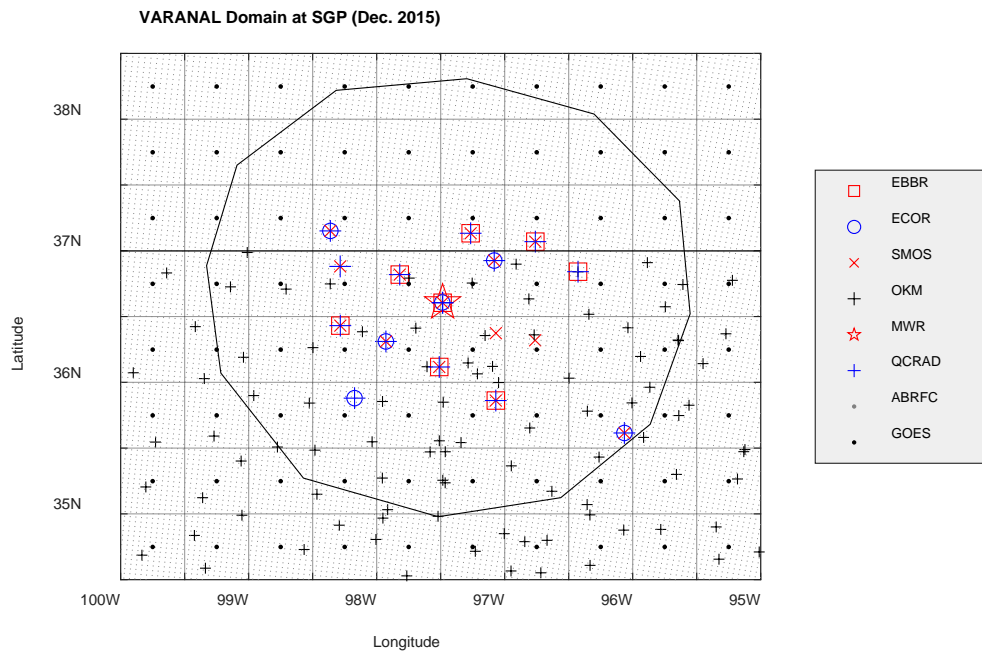
Figure 4. ARM surface stations, GOES TOA measurements, and ABRFC gridded precipitation data at the SGP domain as of December. Gray lines show $0.5° \times 0.5°$ s grids of GOES satellite products (black dots). The black circle is the domain of VARANAL. Black line at 37°N indicates the boundary between Oklahoma (below) and Kansas (above). (Revised from Tang et al. [2016a]).

To avoid overweighting problem due to the spatial distribution of surface stations, the surface stational measurements are firstly interpolated into the GOES grids of $0.5° \times 0.5°$ horizontal resolution in the domain in Figure 4. If there are actual measurements within the $0.5° \times 0.5°$ grid box, simple arithmetic averaging is used to obtain the value for that grid box. Under circumstances when multiple instruments observe the same quantities, their measurements are merged in the arithmetic averaging process with a weighting function depending on their quality. If there is no actual measurement in the grid box, the Barnes scheme (Barnes 1964) is used with the length scale of L_x=50km, L_y=50km, and L_t=6hr to fill the missing grid box. Then, the constraint variables are calculated by averaging the interpolated fields within the VARANAL domain (the dodecagon in Figure 4).

Note that there are periods when RUC/RAP data are missing. The missing RUC/RAP data with gap > 6hr, listed in Table 1, are filled with RUC/RAP data at another time periods of the month. Missing periods < 6hr are filled by linear interpolation. Please be careful when using the continuous forcing data during these periods.

Table 1.   Time periods of missing RUC/RAP data with gap > 6hr.

Data source	Year	Missing period
RAP	2014	Dec. 19 15Z to Dec. 19 23Z
RAP	2014	Dec. 20 20Z to Dec. 21 19Z
RAP	2014	Dec. 25 20Z to Dec. 26 19Z
RAP	2016	May 16 14Z to May 17 23Z
RAP	2018	Feb. 18 00Z to Feb. 18 23Z
RAP	2018	Apr. 10 01Z to Apr. 10 23Z
RAP	2018	May 2 04Z to May 2 23Z
RAP	2018	May 7 03Z to May 7 23Z

3.3   Output Data

The final outputs from the variational analysis for the single-level time series and multi-layer data include forcing data for SCM/CRM/LES and evaluation data. All the output variables are listed in the file head of the output file given in Appendix 1.

4.0   Data Products

Table 2 lists the available field campaigns (updated in May 2019) and the data sources used to derive these forcings. All the forcing data, as well as their readme files including the field campaign background, VARANAL settings, input data sources, and version information, can be downloaded from https://iop.archive.arm.gov/arm-iop/0eval-data/xie/scm-forcing/.

Table 2.   Information of large-scale forcing for field campaigns.

Campaigns	Site	Time	Data sources	References
9704	SGP	Apr. 1997	Radiosonde supplemented with RUC and wind profiler, ARM surface measurements, GOES TOA fluxes	Zhang and Lin 1997; Zhang et al. 2001b
9706	SGP	Jun. 1997	Radiosonde supplemented with RUC and wind profiler, ARM surface measurements, GOES TOA fluxes	Xie et al. 2002
9709	SGP	Sep. 1997	Radiosonde supplemented with RUC and wind profiler, ARM surface measurements, GOES TOA fluxes	Zhang and Lin 1997; Zhang et al. 2001b
9804	SGP	Apr. 1998	Radiosonde supplemented with RUC and wind profiler, ARM surface measurements, GOES TOA fluxes	Zhang and Lin 1997; Zhang et al. 2001b
9901	SGP	Jan. 1999	Radiosonde supplemented with RUC and wind profiler, ARM surface measurements, GOES TOA fluxes	Zhang and Lin 1997; Zhang et al. 2001b

Campaigns	Site	Time	Data sources	References
9903	SGP	Mar. 1999	Radiosonde supplemented with RUC and wind profiler, ARM surface measurements, GOES TOA fluxes	Zhang and Lin 1997; Zhang et al. 2001b
9907	SGP	Jul. 1999	Radiosonde supplemented with RUC and wind profiler, ARM surface measurements, GOES TOA fluxes	Zhang and Lin 1997; Zhang et al. 2001b
0003	SGP	Mar. 2000	Radiosonde supplemented with RUC and wind profiler, ARM surface measurements, GOES TOA fluxes	Xie et al. 2005
0009	SGP	Sep. 2000	Radiosonde supplemented with RUC and wind profiler, ARM surface measurements, GOES TOA fluxes	Zhang and Lin 1997; Zhang et al. 2001b
0011	SGP	Nov. 2000	Radiosonde supplemented with RUC and wind profiler, ARM surface measurements, GOES TOA fluxes	Zhang and Lin 1997; Zhang et al. 2001b
0205	SGP	May. 2002	Radiosonde supplemented with RUC and wind profiler, ARM surface measurements, GOES TOA fluxes	Zhang and Lin 1997; Zhang et al. 2001b
0211	SGP	Nov. 2002	Radiosonde supplemented with RUC and wind profiler, ARM surface measurements, GOES TOA fluxes	Zhang and Lin 1997; Zhang et al. 2001b
0305	SGP	May. 2003	Radiosonde supplemented with RUC and wind profiler, ARM surface measurements, GOES TOA fluxes	Zhang and Lin 1997; Zhang et al. 2001b
Continuous forcing at Darwin	TWP	Wet seasons 2004-2007	Radiosonde with ERA-Interim reanalysis as background, radar precipitation, ARM MWR liquid water path (LWP), surface, and TOA heat and radiative fluxes from ERA-Interim	Davies et al. 2013
Mixed-Phase Arctic Cloud Experiment (M-PACE)	North Slope of Alaska (NSA)	5-22 Oct 2004	Radiosonde with ERA-Interim reanalysis as background, satellite TOA fluxes, surface stations for precipitation, LWP and radiative fluxes; turbulence fluxes come from bulk calculation for land and ERA-Interim reanalysis for ocean.	Xie et al. 2006
Tropical Warm Pool-International Cloud Experiment (TWP-ICE)	TWP	Jan-Feb 2006	Radiosonde, satellite TOA fluxes, radar precipitation, surface fluxes measured from ship and land stations. ERA-Interim data are used as background and to fill missing gaps.	Xie et al. 2010
Cloud and Land Surface Interaction Campaign (CLASIC)	SGP	June 2007	Radiosonde with RUC as background. ARM surface measurements, GOES TOA fluxes	
Indirect and Semi-Direct Aerosol Campaign (ISDAC)	NSA	Apr 2008	Purely based on ERA-Interim	Xie et al. 2004

Campaigns	Site	Time	Data sources	References
AMF CHINA	HFE	Nov 2008	MERRA reanalysis, Tropical Rainfall Measuring Mission (TRMM) precipitation, satellite TOA fluxes, surface stations for meteorology variables and surface fluxes	Xie et al. 2004
Midlatitude Continental Convective Clouds (MC3E)	SGP	Apr-Jun 2011	Radiosonde with RUC as background. ARM surface measurements, GOES TOA fluxes	Xie et al. 2014
ARM Madden-Julian Oscillation (MJO) Investigation Experiment-Gan Island (AMIE-GAN)	GAN	Oct 2011-Mar 2012	ECMWF analysis (state variables, turbulence and radiative fluxes), Shared Mobile Atmospheric Research and Teaching Radar (SMART-R), S-band dual-polarimetric radar (S-POL), and TRMM radar precipitation	Ciesielski et al. 2017
Dynamics of the Madden-Julian Oscillation (DYNAMO)-Revelle	REV	Oct-Dec 2011	ECMWF analysis (state variables, turbulence and radiative fluxes), Colorado State University (CSU) Tropical Ocean Global Atmosphere (TOGA) radar and TRMM precipitation	Ciesielski et al. 2017
DYNAMO-North Sounding Array		Oct-Dec 2011	Gridded sounding data from CSU, TRMM precipitation, ECMWF analysis for surface and TOA heat and radiative fluxes	Ciesielski et al. 2017
GOAmazon 2014/15	MAO	Jan 2014-Dec 2015	ERA-Interim reanalysis, Sistema de Proteção da Amazônia (SIPAM) radar precipitation, TRMM precipitation, GOES TOA fluxes, ARM and Brazilian surface stations for radiative and turbulent fluxes	Tang et al. 2016b
Plains Elevated Convection at Night (PECAN)	SGP	Jun-Jul 2017	Radiosonde with RUC as background. ARM and PECAN surface measurements, GOES TOA fluxes.	

5.0 Contacts

Shuaiqi Tang
Atmospheric, Earth, and Energy Division (L-103)
Lawrence Livermore National Laboratory
Livermore, California 94550
tang32@llnl.gov

Cheng Tao
Atmospheric, Earth, and Energy Division (L-103)
Lawrence Livermore National Laboratory
Livermore, CA 94550
tao4@llnl.gov

Shaocheng Xie
Atmospheric, Earth, and Energy Division (L-103)
Lawrence Livermore National Laboratory
Livermore, CA 94550
xie2@llnl.gov

6.0 References

Barnes, SL. 1964. "A Technique for Maximizing Details in Numerical Weather Map Analysis." *Journal of Applied Meteorology* 3(4): 396–409,
https://doi.org/10.1175/1520- 0450(1964)003<0396:ATFMDI>2.0.CO;2

Ciesielski, PE, RH Johnson, X Jiang, Y Zhang, and S Xie. 2017. "Relationships between radiation, clouds, and convection during DYNAMO." *Journal of Geophysical Research – Atmospheres* 122(5): 2529–2548, https://doi.org/10.1002/2016JD025965

Cook, DR. 2019a. Eddy Correlation Flux Measurement System (ECOR) Instrument Handbook. U.S. Department of Energy. DOE/SC-ARM/TR-052.

Cook, DR, and RC Sullivan. 2019b. Energy Balance Bowen Ratio (EBBR) Instrument Handbook. U.S. Department of Energy. DOE/SC-ARM/TR-037.

Cressman, GP. 1959. "An Operational Objective Analysis System." *Monthly Weather Review* 87(10): 367–374, https://doi.org/10.1175/1520-0493(1959)087<0367:AOOAS>2.0.CO;2

Davies, L, C Jakob, K Cheung, A Del Genio, A Hill, T Hume, RJ Keane, T Komori, VE Larson, Y Lin, X Liu, BJ Nielsen, J Petch, RS Plant, MS Singh, X Shi, X Song, W Wang, MA Whitall A Wolf, S Xie, and G Zhang. 2013. "A single-column model ensemble approach applied to the TWP-ICE experiment." *Journal of Geophysical Research – Atmospheres* 118(12): 6544–6563, https://doi.org/10.1002/jgrd.50450

Tang, S, and M Zhang. 2015. "Three-dimensional constrained variational analysis: Approach and application to analysis of atmospheric diabatic heating and derivative fields during an ARM SGP intensive observational period." *Journal of Geophysical Research – Atmospheres* 120(15): 7283–7299, https://doi.org/10.1002/2015JD023621

Tang, S, M Zhang, and S Xie. 2016a. "An ensemble constrained variational analysis of atmospheric forcing data and its application to evaluate clouds in CAM5." *Journal of Geophysical Research – Atmospheres* 121(1): 33–48, https://doi.org/10.1002/2015JD024167

Tang, S, S Xie, M Zhang, Q Tang, Y Zhang, SA Klein, DR Cook, and RC Sullivan. 2019. "Differences in Eddy-Correlation and Energy-Balance Surface Turbulent Heat Flux Measurements and Their Impacts on the Large-Scale Forcing Fields at the ARM SGP Site." *Journal of Geophysical Research – Atmospheres* 124(6): 3301–3318, https://doi.org/10.1029/2018jd029689

Tang, S, S Xie, Y Zhang, M Zhang, C Schumacher, H Upton, MP Jensen, KL Johnson, M Wang, M Ahlgrimm, Z Feng, P Minnis, and M Thieman. 2016b. "Large-scale vertical velocity, diabatic heating and drying profiles associated with seasonal and diurnal variations of convective systems observed in the GoAmazon2014/5 experiment." *Atmospheric Chemistry and Physics* 16(22): 14249–14264, https://doi.org/10.5194/acp-16-14249-2016

Xie, S, RT Cederwall, and M Zhang. 2004. "Developing long-term single-column model/cloud system–resolving model forcing data using numerical weather prediction products constrained by surface and top of the atmosphere observations." *Journal of Geophysical Research – Atmospheres* 109(D1): D01104, https://doi.org/10.1029/2003jd004045

Xie, S, SA Klein, M Zhang, JJ Yio, RT Cederwall, and R McCoy. 2006. "Developing large-scale forcing data for single-column and cloud-resolving models from the Mixed-Phase Arctic Cloud Experiment." *Journal of Geophysical Research – Atmospheres* 111(D19): D19104, https://doi.org/10.1029/2005jd006950

Xie, S, T Hume, C Jakob, SA Klein, RB McCoy, and M Zhang. 2010. "Observed Large-Scale Structures and Diabatic Heating and Drying Profiles during TWP-ICE." *Journal of Climate* 23(1): 57–79, https://doi.org/10.1175/2009jcli3071.1

Xie, S, Y Zhang, SE Giangrande, MP Jensen, R McCoy, and M Zhang. 2014. "Interactions between cumulus convection and its environment as revealed by the MC3E sounding array." *Journal of Geophysical Research – Atmospheres* 119(20): 11784–11808, https://doi.org/10.1002/2014JD022011

Xie, S, K-M Xu, RT Cederwall, P Bechtold, AD Del Genio, SA Klein, DG Cripe, SJ Ghan, D Gregory, SF Iacobellis, SK Krueger, U Lohmann, JC Petch, DA Randall, LD Rotstayn, RCJ Somerville, YC Sud, K Von Salzen, GK Walker, A Wolf, JJ Yio, GJ Zhang, and M Zhang. 2002. "Intercomparison and evaluation of cumulus parametrizations under summertime midlatitude continental conditions." *Quarterly Journal of the Royal Meteorological Society* 128(582): 1095–1135, https://doi.org/10.1256/003590002320373229

Xie, S, M Zhang, M Branson, RT Cederwall, AD Del Genio, ZA Eitzen, SJ Ghan, SF Iacobellis, KL Johnson, M Khairoutdinov, SA Klein, SK Krueger, W Lin, U Lohmann, MA Miller, DA Randall, RCJ Somerville, YC Sud, GK Walker, A Wolf, X Wu, K-M Xu, JJ Yio, G Zhang, and J Zhang. 2005. "Simulations of midlatitude frontal clouds by single-column and cloud-resolving models during the Atmospheric Radiation Measurement March 2000 cloud intensive operational period." *Journal of Geophysical Research – Atmospheres* 110(D15): D15S03, https://doi.org/10.1029/2004JD005119

Zhang, M, and J Lin. 1997. "Constrained Variational Analysis of Sounding Data Based on Column-Integrated Budgets of Mass, Heat, Moisture, and Momentum: Approach and Application to ARM Measurements." *Journal of the Atmospheric Sciences* 54(11): 1503–1524, https://doi.org/10.1175/1520- 0469(1997)054<1503:CVAOSD>2.0.CO;2

Zhang, M, RCJ Somerville, and S Xie. 2016. "The SCM Concept and Creation of ARM Forcing Datasets." *Meteorological Monographs* 57: 24.21–24.12, https://doi.org/10.1175/AMSMONOGRAPHS-D-15-0040.1

Zhang, M, S Xie, RT Cederwall, and JJ Yio. 2001a. Description of the ARM Operational Objective Analysis System. U.S. Department of Energy. DOE/SC-ARM-TR-005.

Zhang, M, J Lin, RT Cederwall, JJ Yio, and SC Xie. 2001b. "Objective Analysis of ARM IOP Data: Method and Sensitivity." *Monthly Weather Review* 129(2): 295–311, https://doi.org/10.1175/1520- 0493(2001)129<0295:OAOAID>2.0.CO;2

Appendix A

Filehead of Continuous Forcing Data

```
netcdf sgp60varanarapC1.c1.20151201.000000 {
dimensions:
      time = UNLIMITED ; // (744 currently)
      lev = 37 ;
variables:
      double base_time ;
            base_time:units = "seconds since 1970-1-1 0:00:00 0:00" ;
            base_time:long_name = "Base time in Epoch" ;
            base_time:string = "2015-12-1 0:00:00 0:00 GMT" ;
      double time(time) ;
            time:units = "days since 2014-12-31" ;
            time:long_name = "calendar day fraction of the year 2015" ;
            time:calendar = "gregorian" ;
            time:axis = "T" ;
      double time_offset(time) ;
            time_offset:units = "seconds since 2015-12-1 0:00:00 0:00"
;
            time_offset:long_name = "Time offset from base_time" ;
            time_offset:missing_value = 1.e+20f ;
      int year(time) ;
            year:units = " " ;
            year:long_name = "Year" ;
            year:missing_value = -9999s ;
      int month(time) ;
            month:units = " " ;
            month:long_name = "Month" ;
            month:missing_value = -9999s ;
      int day(time) ;
            day:units = " " ;
            day:long_name = "Day" ;
            day:missing_value = -9999s ;
      int hour(time) ;
            hour:units = " " ;
            hour:long_name = "Hour" ;
            hour:missing_value = -9999s ;
      int minute(time) ;
            minute:units = "Minute" ;
            minute:long_name = " " ;
```

```
            minute:missing_value = -9999s ;
      float lat ;
            lat:units = "degrees_north" ;
            lat:long_name = "latitude" ;
      float lon ;
            lon:units = "degrees_west" ;
            lon:long_name = "longitude " ;
      float alt ;
            alt:units = "m" ;
            alt:long_name = "altitude, height above mean sea level" ;
      float phis ;
            phis:units = "m2/s2" ;
            phis:long_name = "surface geopential height" ;
      float lev(lev) ;
            lev:units = "mb" ;
            lev:long_name = "pressure levels" ;
      float T(time, lev) ;
            T:units = "K" ;
            T:long_name = "Temperature" ;
            T:standard_name = "air_temperature" ;
            T:version = "v2" ;
            T:source = "RAP Analysis" ;
            T:missing_value = -9999.f ;
      float q(time, lev) ;
            q:units = "g/kg" ;
            q:long_name = "Water vapor mixing ratio" ;
            q:standard_name = "humidity_mixing_ratio" ;
            q:version = "v2" ;
            q:source = "RAP Analysis" ;
            q:missing_value = -9999.f ;
      float u(time, lev) ;
            u:units = "m/s" ;
            u:long_name = "Horizontal wind U component" ;
            u:standard_name = "eastward_wind" ;
            u:version = "v2" ;
            u:source = "RAP Analysis" ;
            u:missing_value = -9999.f ;
      float v(time, lev) ;
            v:units = "m/s" ;
            v:long_name = "Horizontal wind V component" ;
            v:standard_name = "northward_wind" ;
            v:version = "v2" ;
            v:source = "RAP Analysis" ;
            v:missing_value = -9999.f ;
      float omega(time, lev) ;
            omega:units = "mb/hour" ;
            omega:long_name = "vertical velocity" ;
            omega:standard_name =
"lagrangian_tendency_of_air_pressure" ;
            omega:version = "v2" ;
            omega:source = "Derived from RAP Analysis" ;
            omega:missing_value = -9999.f ;
```

A.2

```
    float div(time, lev) ;
        div:units = "1/s" ;
        div:long_name = "Horizontal wind divergence" ;
        div:standard_name = "divergence_of_wind" ;
        div:version = "v2" ;
        div:source = "Derived from RAP Analysis" ;
        div:missing_value = -9999.f ;
    float T_adv_h(time, lev) ;
        T_adv_h:units = "K/hour" ;
        T_adv_h:long_name = "Horizontal Temp advection" ;
        T_adv_h:standard_name =
"tendency_of_air_temperature_due_to_advection horizontal" ;
        T_adv_h:version = "v2" ;
        T_adv_h:source = "Derived from RAP Analysis" ;
        T_adv_h:missing_value = -9999.f ;
    float T_adv_v(time, lev) ;
        T_adv_v:units = "K/hour" ;
        T_adv_v:long_name = "Vertical Temp advection" ;
        T_adv_v:standard_name =
"tendency_of_air_temperature_due_to_advection vertical" ;
        T_adv_v:version = "v2" ;
        T_adv_v:source = "Derived from RAP Analysis" ;
        T_adv_v:missing_value = -9999.f ;
    float q_adv_h(time, lev) ;
        q_adv_h:units = "g/kg/hour" ;
        q_adv_h:long_name = "Horizontal q advection" ;
        q_adv_h:standard_name =
"tendency_of_humidity_mixing_ratio_due_to_advection horizontal" ;
        q_adv_h:version = "v2" ;
        q_adv_h:source = "Derived from RAP Analysis" ;
        q_adv_h:missing_value = -9999.f ;
    float q_adv_v(time, lev) ;
        q_adv_v:units = "g/kg/hour" ;
        q_adv_v:long_name = "Vertical q advection" ;
        q_adv_v:standard_name =
"tendency_of_humidity_mixing_ratio_due_to_advection vertical" ;
        q_adv_v:version = "v2" ;
        q_adv_v:source = "Derived from RAP Analysis" ;
        q_adv_v:missing_value = -9999.f ;
    float s(time, lev) ;
        s:units = "K" ;
        s:long_name = "Dry satic energy/Cp" ;
        s:standard_name =
"dry_static_energy_content_of_atmosphere_layer" ;
        s:version = "v2" ;
        s:source = "RAP Analysis" ;
        s:missing_value = -9999.f ;
    float s_adv_h(time, lev) ;
        s_adv_h:units = "K/hour" ;
        s_adv_h:long_name = "Hori. dry static energy adv./Cp" ;
        s_adv_h:standard_name =
"tendency_of_dry_static_energy_due_to_advection horizontal" ;
```

```
            s_adv_h:version = "v2" ;
            s_adv_h:source = "Derived from RAP Analysis" ;
            s_adv_h:missing_value = -9999.f ;
     float s_adv_v(time, lev) ;
            s_adv_v:units = "K/hour" ;
            s_adv_v:long_name = "Vert. dry static energy adv./Cp" ;
            s_adv_v:standard_name =
"tendency_of_dry_static_energy_due_to_advection vertical" ;
            s_adv_v:version = "v2" ;
            s_adv_v:source = "Derived from RAP Analysis" ;
            s_adv_v:missing_value = -9999.f ;
     float dsdt(time, lev) ;
            dsdt:units = "K/hour" ;
            dsdt:long_name = "d(dry static energy)/dt/Cp" ;
            dsdt:standard_name =
"tendency_of_dry_static_energy_content_of_atmosphere_layer" ;
            dsdt:version = "v2" ;
            dsdt:source = "RAP Analysis" ;
            dsdt:missing_value = -9999.f ;
     float dTdt(time, lev) ;
            dTdt:units = "K/hour" ;
            dTdt:long_name = "d(temperature)/dt" ;
            dTdt:standard_name = "tendency_of_air_temperature" ;
            dTdt:version = "v2" ;
            dTdt:source = "RAP Analysis" ;
            dTdt:missing_value = -9999.f ;
     float dqdt(time, lev) ;
            dqdt:units = "g/kg/hour" ;
            dqdt:long_name = "d(water vapor mixing ratio)/dt" ;
            dqdt:standard_name = "tendency_of_humidity_mixing_ratio" ;
            dqdt:version = "v2" ;
            dqdt:source = "RAP Analysis" ;
            dqdt:missing_value = -9999.f ;
     float q1(time, lev) ;
            q1:units = "K/hour" ;
            q1:long_name = "Apparent heat sources Yanai (1973)" ;
            q1:standard_name = "Q1" ;
            q1:version = "v2" ;
            q1:source = "Derived from RAP Analysis" ;
            q1:missing_value = -9999.f ;
     float q2(time, lev) ;
            q2:units = "K/hour" ;
            q2:long_name = "Apparent moisture sinks Yanai (1973)" ;
            q2:standard_name = "Q2" ;
            q2:version = "v2" ;
            q2:source = "Derived from RAP Analysis" ;
            q2:missing_value = -9999.f ;
     float prec_srf(time) ;
            prec_srf:units = "mm/hour" ;
            prec_srf:long_name = "Surface precipitation" ;
            prec_srf:standard_name = "lwe_precipitation_rate" ;
            prec_srf:version = "v2" ;
```

```
            prec_srf:source = "Rain gauge adjusted WSR-88D radar
precipitation - ABRFC" ;
            prec_srf:missing_value = -9999.f ;
      float LH(time) ;
            LH:units = "W/m2" ;
            LH:long_name = "Surf. latent heat flux, upward positive" ;
            LH:standard_name = "surface_upward_latent_heat_flux" ;
            LH:version = "v2" ;
            LH:source = "Merged from BAEBBR and QCECOR" ;
            LH:missing_value = -9999.f ;
      float SH(time) ;
            SH:units = "W/m2" ;
            SH:long_name = "Surf. sensible heat flux,upward positive" ;
            SH:standard_name = "surface_upward_sensible_heat_flux" ;
            SH:version = "v2" ;
            SH:source = "Merged from BAEBBR and QCECOR" ;
            SH:missing_value = -9999.f ;
      float p_srf_aver(time) ;
            p_srf_aver:units = "mb" ;
            p_srf_aver:long_name = "Surf. pressure averaged over the
domain" ;
            p_srf_aver:standard_name = "surface_air_pressure domain
average" ;
            p_srf_aver:version = "v2" ;
            p_srf_aver:source = "Merged products from surface
measurements - SMOS, OKM, KAS mesonet" ;
            p_srf_aver:missing_value = -9999.f ;
      float p_srf_center(time) ;
            p_srf_center:units = "mb" ;
            p_srf_center:long_name = "Surf. pressure at center of the
domain" ;
            p_srf_center:standard_name = "surface_air_pressure domain
center" ;
            p_srf_center:version = "v2" ;
            p_srf_center:source = "Merged products from surface
measurements - SMOS, OKM, KAS mesonet" ;
            p_srf_center:missing_value = -9999.f ;
      float T_srf(time) ;
            T_srf:units = "C" ;
            T_srf:long_name = "Surf. air temperature" ;
            T_srf:standard_name = "air_temperature at 2m" ;
            T_srf:version = "v2" ;
            T_srf:source = "Merged products from surface measurements -
SMOS, OKM, KAS mesonet" ;
            T_srf:missing_value = -9999.f ;
      float T_soil(time) ;
            T_soil:units = "C" ;
            T_soil:long_name = "Soil temperature" ;
            T_soil:standard_name = "soil_temperature" ;
            T_soil:version = "v2" ;
            T_soil:source = "BAEBBR" ;
            T_soil:missing_value = -9999.f ;
```

A.5

```
     float RH_srf(time) ;
           RH_srf:units = "%" ;
           RH_srf:long_name = "Surf. air relative humidity" ;
           RH_srf:standard_name = "relative_humidity at 2m" ;
           RH_srf:version = "v2" ;
           RH_srf:source = "Merged products from surface measurements
- SMOS, OKM, KAS mesonet" ;
           RH_srf:missing_value = -9999.f ;
     float wspd_srf(time) ;
           wspd_srf:units = "m/s" ;
           wspd_srf:long_name = "Surf. wind speed" ;
           wspd_srf:standard_name = "wind_speed at 10m" ;
           wspd_srf:version = "v2" ;
           wspd_srf:source = "Merged products from surface
measurements - SMOS, OKM, KAS mesonet" ;
           wspd_srf:missing_value = -9999.f ;
     float u_srf(time) ;
           u_srf:units = "m/s" ;
           u_srf:long_name = "Surf. U component" ;
           u_srf:standard_name = "eastward_wind at 10m" ;
           u_srf:version = "v2" ;
           u_srf:source = "Merged products from surface measurements -
SMOS, OKM, KAS mesonet" ;
           u_srf:missing_value = -9999.f ;
     float v_srf(time) ;
           v_srf:units = "m/s" ;
           v_srf:long_name = "Surf. V component" ;
           v_srf:standard_name = "northward_wind at 10m" ;
           v_srf:version = "v2" ;
           v_srf:source = "Merged products from surface measurements -
SMOS, OKM, KAS mesonet" ;
           v_srf:missing_value = -9999.f ;
     float rad_net_srf(time) ;
           rad_net_srf:units = "W/m2" ;
           rad_net_srf:long_name = "Surf. net rad., Downward" ;
           rad_net_srf:standard_name = "Surf. net rad., Downward" ;
           rad_net_srf:version = "v2" ;
           rad_net_srf:source = "SIRS - qcrad" ;
           rad_net_srf:missing_value = -9999.f ;
     float lw_net_toa(time) ;
           lw_net_toa:units = "W/m2" ;
           lw_net_toa:long_name = "TOA LW flux, upward positive" ;
           lw_net_toa:standard_name = "toa_net_upward_longwave_flux" ;
           lw_net_toa:version = "v2" ;
           lw_net_toa:source = "GOES VISST" ;
           lw_net_toa:missing_value = -9999.f ;
     float sw_net_toa(time) ;
           sw_net_toa:units = "W/m2" ;
           sw_net_toa:long_name = "TOA net SW flux, downward positive"
;
           sw_net_toa:standard_name =
"toa_net_downward_shortwave_flux" ;
```

```
        sw_net_toa:version = "v2" ;
        sw_net_toa:source = "GOES VISST" ;
        sw_net_toa:missing_value = -9999.f ;
float sw_dn_toa(time) ;
        sw_dn_toa:units = "W/m2" ;
        sw_dn_toa:long_name = "TOA solar insolation" ;
        sw_dn_toa:standard_name = "TOA solar insolation" ;
        sw_dn_toa:version = "v2" ;
        sw_dn_toa:source = "GOES VISST" ;
        sw_dn_toa:missing_value = -9999.f ;
float cld_low(time) ;
        cld_low:units = "%" ;
        cld_low:long_name = "Satellite-measured low level cloud" ;
        cld_low:standard_name = " " ;
        cld_low:version = "v2" ;
        cld_low:source = "GOES VISST" ;
        cld_low:missing_value = -9999.f ;
float cld_mid(time) ;
        cld_mid:units = "%" ;
        cld_mid:long_name = "Satellite-measured middle level cloud"
;
        cld_mid:standard_name = " " ;
        cld_mid:version = "v2" ;
        cld_mid:source = "GOES VISST" ;
        cld_mid:missing_value = -9999.f ;
float cld_high(time) ;
        cld_high:units = "%" ;
        cld_high:long_name = "Satellite-measured high level cloud"
;
        cld_high:standard_name = " " ;
        cld_high:version = "v2" ;
        cld_high:source = "GOES VISST" ;
        cld_high:missing_value = -9999.f ;
float cld_tot(time) ;
        cld_tot:units = "%" ;
        cld_tot:long_name = "Satellite-measured total cloud" ;
        cld_tot:standard_name = " " ;
        cld_tot:version = "v2" ;
        cld_tot:source = "GOES VISST" ;
        cld_tot:missing_value = -9999.f ;
float cld_thick(time) ;
        cld_thick:units = "km" ;
        cld_thick:long_name = "Satellite-measured cloud thickness"
;
        cld_thick:standard_name = " " ;
        cld_thick:version = "v2" ;
        cld_thick:source = "GOES VISST" ;
        cld_thick:missing_value = -9999.f ;
float cld_top(time) ;
        cld_top:units = "km" ;
        cld_top:long_name = "Satellite-measured cloud top" ;
        cld_top:standard_name = "cloud_top_altitude" ;
```

```
        cld_top:version = "v2" ;
        cld_top:source = "GOES VISST" ;
        cld_top:missing_value = -9999.f ;
float LWP(time) ;
        LWP:units = "cm" ;
        LWP:long_name = "cloud liquid water path" ;
        LWP:standard_name = "atmosphere_cloud_liquid_water_content"
;
        LWP:version = "v2" ;
        LWP:source = "MWR" ;
        LWP:missing_value = -9999.f ;
float dh2odt_col(time) ;
        dh2odt_col:units = "mm/hour" ;
        dh2odt_col:long_name = "Column-integrated dH2O/dt" ;
        dh2odt_col:standard_name = " " ;
        dh2odt_col:version = "v2" ;
        dh2odt_col:source = "RAP Analysis" ;
        dh2odt_col:missing_value = -9999.f ;
float h2o_adv_col(time) ;
        h2o_adv_col:units = "mm/hour" ;
        h2o_adv_col:long_name = "Column-integrated H2O adv." ;
        h2o_adv_col:standard_name = " " ;
        h2o_adv_col:version = "v2" ;
        h2o_adv_col:source = "RAP Analysis" ;
        h2o_adv_col:missing_value = -9999.f ;
float evap_srf(time) ;
        evap_srf:units = "mm/hour" ;
        evap_srf:long_name = "Surface evaporation" ;
        evap_srf:standard_name = "lwe_water_evaporation_rate at
surface" ;
        evap_srf:version = "v2" ;
        evap_srf:source = "Derived from LH" ;
        evap_srf:missing_value = -9999.f ;
float dsdt_col(time) ;
        dsdt_col:units = "W/m2" ;
        dsdt_col:long_name = "Column d(dry static energy)/dt" ;
        dsdt_col:standard_name = " " ;
        dsdt_col:version = "v2" ;
        dsdt_col:source = "RAP Analysis" ;
        dsdt_col:missing_value = -9999.f ;
float s_adv_col(time) ;
        s_adv_col:units = "W/m2" ;
        s_adv_col:long_name = "Column dry static energy adv." ;
        s_adv_col:standard_name = " " ;
        s_adv_col:version = "v2" ;
        s_adv_col:source = "RAP Analysis" ;
        s_adv_col:missing_value = -9999.f ;
float rad_heat_col(time) ;
        rad_heat_col:units = "W/m2" ;
        rad_heat_col:long_name = "Column radiative heating" ;
        rad_heat_col:standard_name = " " ;
        rad_heat_col:version = "v2" ;
```

```
            rad_heat_col:source = "Surface and TOA radiation
measurements" ;
            rad_heat_col:missing_value = -9999.f ;
      float LH_col(time) ;
            LH_col:units = "W/m2" ;
            LH_col:long_name = "Column latent heating" ;
            LH_col:standard_name = " " ;
            LH_col:version = "v2" ;
            LH_col:source = "Derived from surface precipitation" ;
            LH_col:missing_value = -9999.f ;
      float omega_srf(time) ;
            omega_srf:units = "mb/hr" ;
            omega_srf:long_name = "Surface omega" ;
            omega_srf:standard_name =
"lagrangian_tendency_of_air_pressure at surface" ;
            omega_srf:version = "v2" ;
            omega_srf:source = "set to zero" ;
            omega_srf:missing_value = -9999.f ;
      float q_srf(time) ;
            q_srf:units = "kg/kg" ;
            q_srf:long_name = "water vapor mixing ratio" ;
            q_srf:standard_name = "humidity_mixing_ratio at 2m" ;
            q_srf:version = "v2" ;
            q_srf:source = "Merged products from surface measurements -
SMOS, OKM, KAS mesonet" ;
            q_srf:missing_value = -9999.f ;
      float s_srf(time) ;
            s_srf:units = "K" ;
            s_srf:long_name = "dry static energy/Cp" ;
            s_srf:standard_name = "dry_static_energy at 2m" ;
            s_srf:version = "v2" ;
            s_srf:source = "Merged products from surface measurements -
SMOS, OKM, KAS mesonet" ;
            s_srf:missing_value = -9999.f ;
      float PW(time) ;
            PW:units = "cm" ;
            PW:long_name = "column precip_water" ;
            PW:standard_name =
"tendency_of_atmosphere_water_vapor_content" ;
            PW:version = "v2" ;
            PW:source = "MWR" ;
            PW:missing_value = -9999.f ;
      float lw_up_srf(time) ;
            lw_up_srf:units = "W/m2" ;
            lw_up_srf:long_name = "Surf. upwelling LW" ;
            lw_up_srf:standard_name =
"surface_upwelling_longwave_flux_in_air" ;
            lw_up_srf:version = "v2" ;
            lw_up_srf:source = "SIRS - qcrad" ;
            lw_up_srf:missing_value = -9999.f ;
      float lw_dn_srf(time) ;
            lw_dn_srf:units = "W/m2" ;
```

```
        lw_dn_srf:long_name = "Surf. downwelling LW" ;
        lw_dn_srf:standard_name =
"surface_downwelling_longwave_flux_in_air" ;
        lw_dn_srf:version = "v2" ;
        lw_dn_srf:source = "SIRS - qcrad" ;
        lw_dn_srf:missing_value = -9999.f ;
    float sw_up_srf(time) ;
        sw_up_srf:units = "W/m2" ;
        sw_up_srf:long_name = "Surf. upwelling SW" ;
        sw_up_srf:standard_name =
"surface_upwelling_shortwave_flux_in_air" ;
        sw_up_srf:version = "v2" ;
        sw_up_srf:source = "SIRS - qcrad" ;
        sw_up_srf:missing_value = -9999.f ;
    float sw_dn_srf(time) ;
        sw_dn_srf:units = "W/m2" ;
        sw_dn_srf:long_name = "Surf. downwelling SW" ;
        sw_dn_srf:standard_name =
"surface_downwelling_shortwave_flux_in_air" ;
        sw_dn_srf:version = "v2" ;
        sw_dn_srf:source = "SIRS - qcrad" ;
        sw_dn_srf:missing_value = -9999.f ;
    float T_skin(time) ;
        T_skin:units = "C" ;
        T_skin:long_name = "Surf. skin temperature" ;
        T_skin:standard_name = "surface_temperature" ;
        T_skin:version = "v2" ;
        T_skin:source = "derived from srface LW with emissivisity
0.98" ;
        T_skin:missing_value = -9999.f ;


// global attributes:
        :Conventions = "CF-1.7" ;
        :title = "VarAna 1hr RAP_Based v2: SGP 2015-12" ;
        :history = "Version: v2" ;
        :update = "surface LH and SH are merged from ECOR and EBBR
instruments" ;
        :date_created = "Fri Apr 14 06:02:44 2017" ;
        :contact = "Shuaiqi Tang: tang32@llnl.gov, Qi Tang:
tang30@llnl.gov, Yunyan Zhang: zhang25@llnl.gov and Shaocheng Xie:
xie2@llnl.gov" ;
        :program_name = "proc_output_nwp.pro" ;
        :institution = "Lawrence Livermore National Laboratory, CA,
USA" ;
        :references = "https://www.arm.gov/data/data-
sources/varanal-29" ;
        :note = "Data below the surface are set to lowest available
level data" ;
}
```